Biodistribution and Radiation Dosimetry of the Dopamine D_2 Ligand ^{11}C-Raclopride Determined from Human Whole-Body PET

Mark Slifstein, PhD[1,2]; Dah-Ren Hwang, PhD[1–3]; Diana Martinez, MD[1,2]; Jesper Ekelund, MD, PhD[1,2]; Yiyun Huang, PhD[1–3]; Elizabeth Hackett, BBA, RT(n)[1,2]; Anissa Abi-Dargham, MD[1,2]; and Marc Laruelle, MD[1–3]

[1]*Department of Psychiatry, Columbia University, New York, New York;* [2]*Division of Functional Brain Mapping, New York State Psychiatric Institute, New York, New York; and* [3]*Department of Radiology, Columbia University, New York, New York*

Whole-body radiation dosimetry of ^{11}C-raclopride was performed in healthy human volunteers. **Methods:** Subjects (n = 6) were scanned with PET. Subjects received single-bolus injections of ^{11}C-raclopride (*S*-(−)-3,5-dichloro-*N*-[(1-ethyl-2-pyrrolidinyl)]methyl-2-hydroxy-6-methoxybenzamide) (533 ± 104 MBq) and were scanned for approximately 110 min with a 2-dimensional whole-body protocol. Regions of interest were placed over all visually identifiable organs and time–activity curves were generated. Residence times were computed as the area under the curve of the time–activity curves, normalized to injected activities and standard values of organ volumes. Absorbed doses were computed according to the MIRD schema with MIRDOSE3.1 software. **Results:** Organs with the highest radiation burden were gallbladder wall, small intestine, liver, and urinary bladder wall. **Conclusion:** On the basis of the estimated absorbed dose, the maximum allowable single study dose under U.S. federal regulations for studies performed under Radiation Drug Research Committee is 1.58 GBq (42.8 mCi). This is still considerably higher than the doses of ^{11}C-raclopride commonly used in research PET (370−555 MBq).

Key Words: ^{11}C-raclopride; D_2 receptor; dopamine; biodistribution; radiation dosimetry; PET

J Nucl Med 2006; 47:313–319

Raclopride (*S*-(−)-3,5-dichloro-*N*-[(1-ethyl-2-pyrrolidinyl)]methyl-2-hydroxy-6-methoxybenzamide) is a dopamine D_2 receptor antagonist that was originally radiolabeled with ^{11}C (^{11}C-raclopride) for PET in 1985 (*1*) and is suitable for imaging dopamine D_2 receptors in the striatum. Since that time, ^{11}C-raclopride has become one of the most widely used neuroreceptor imaging agents in PET. ^{11}C-Raclopride has been shown to be sensitive to competition from endogenous dopamine (*2,3*), making it suitable for study of the effects of pharmacologic challenges on D_2 parameters as well as those of behavioral tasks designed to elicit the release of dopamine (*4,5*). ^{11}C-Raclopride has been used extensively in a wide range of research studies involving human subjects in which striatal D_2 tone is of interest—for example, in Parkinson's disease (*6–9*), schizophrenia (*10–12*), and substance abuse (*13–17*). Before 2005, ^{11}C-raclopride biodistribution and radiation dosimetry had only been described in 2 abstracts reporting on studies performed on rats (*18*) and rhesus monkeys (*19*). More recently, a study reporting whole-body dosimetry in 3 human subjects has been published (*20*). In the present study we performed whole-body PET scans in 6 healthy adult human volunteers after bolus injections of ^{11}C-raclopride to measure organ activities and estimate radiation-absorbed doses.

MATERIALS AND METHODS

Subjects

Six healthy control subjects (Table 1) participated in the study. The absence of medical, neurologic, and psychiatric history (including alcohol and drug abuse) was assessed by history, review of systems, physical examination, routine blood tests, pregnancy test, urine toxicology, and electrocardiogram. The study was approved by the New York State Psychiatric Institute Institutional Review Board. Subjects provided written informed consent after receiving an explanation of the study.

Radiochemistry

O-Desmethyl raclopride hydrobromide, precursor for the preparation of ^{11}C-raclopride, was obtained from Sigma/Aldrich Chemical Co. ^{11}C-Methyl triflate was produced by passing ^{11}C-methyl iodide through a silver triflate furnace according to Jewett's procedure (*21*). Briefly, $^{11}CO_2$ was bubbled into a tetrahydrofuran solution of lithium aluminum hydride. Concentrated hydrogen iodide was added, and ^{11}C-methyl iodide was distilled through a stream of argon through a silver triflate furnace (195°C) to yield ^{11}C-methyl triflate, which was trapped in a solution of *O*-desmethyl raclopride hydrobromide and sodium hydroxide in dimethyl sulfoxide. After a 5-min reaction at 90°C, the crude product was purified by high-pressure liquid chromatography (column: Phenomenex C_{18}, 10 μm, 25 × 1 cm; solvent: 30% acetonitrile, 70% 0.1 mol/L ammonium formate, and 0.5% acetic acid; flow rate: 10 mL/min). The product fraction was diluted with water and passed through a classic C_{18} Sep-Pak column (Waters). The final

Received Aug. 24, 2005; revision accepted Nov. 7, 2005.

For correspondence or reprints contact: Mark Slifstein, PhD, 1051 Riverside Dr., Unit 31, New York, NY, 10032.

E-mail: mms218@columbia.edu

TABLE 1
Subject Data and Injected Activity of ^{11}C-Raclopride

Subject	Sex	Age (y)	Height (m)	Mass (kg)	Injected dose (MBq)
1	F	34	1.68	74.84	650.83
2	F	21	1.60	62.60	577.61
3	F	30	1.73	72.57	487.66
4	M	35	1.73	103.87	477.67
5	M	34	1.83	81.65	373.33
6	M	26	1.75	68.95	619.01
Mean ± SD		30 ± 5.55	1.72 ± 0.08	77.41 ± 14.42	531.02 ± 103.79

product was recovered from the Sep-Pak column using 1 mL ethanol. The ethanol solution was mixed with saline and filtered through a 0.22-μm filter and collected in a sterile vial.

PET Protocol

Subjects were scanned on the Accel (Siemens) scanner using a whole-body protocol in 2-dimensional (2D) mode. The Accel uses lutetium oxyorthosilicate crystals and has a transaxial full width at half maximum (FWHM) of 6.2 and 6.7 mm at 1 and 10 cm from the center of the field of view and an axial FWHM of 4.3 and 6.0 mm at 0 and 10 cm from the center of the field of view in 2D mode (*22*).

For each subject, there were 7 overlapping bed positions of 14.2-cm length. Before tracer injection and emission scanning, a 5-min transmission scan was acquired for each bed position for subsequent attenuation correction. Emission scanning commenced 1 min after intravenous injection of a single bolus (injected dose = 533 ± 104 MBq [14.4 mCi] ^{11}C-raclopride). Total scan duration was approximately 110 min (the interval between passes varied slightly from scan to scan), collected in 9 passes (7 beds × 15 s, 7 beds × 15 s, 7 beds [7 bed positions] × 30 s, 7 beds × 30 s, 7 beds × 60 s, 7 beds × 60 s, 7 beds × 120 s, 7 beds × 240 s, 7 beds × 240 s). Attenuation corrected data were reconstructed to a grid of 128 × 128 × 196 cubic voxels of 5.1484-mm side length.

Regions of Interest (ROIs)

Organs included in the analysis were determined by visual inspection as those having activity exceeding that of background. ROIs were drawn manually on subsamples of these organs using MEDx software (Sensor Systems) to obtain the mean activity concentration in each region and each pass (within-subject, the same ROIs were applied to data from all passes). Included organs were brain, cortical bone (top of skull), gallbladder contents, heart, liver, lung, small intestine, lower large intestine, kidney, and red marrow (femur). Because the urinary bladder was observed to be isolated from any other tissue with high uptake, an inclusive ROI containing the entire bladder and its contents was used for this organ. The small intestine region was sampled in the duodenum, the area of highest activity in small intestine.

TABLE 2
Residence Times ± SD (n = 6) of ^{11}C-Raclopride for 11 Measured Organs and Remainder of Body

Organ	Residence time (h)
Liver	0.099 ± 0.019
Small intestine	0.081 ± 0.039
Lung	0.040 ± 0.020
Urinary bladder	0.018 ± 0.005
Cortical bone	0.014 ± 0.003
Brain	0.014 ± 0.002
Gallbladder	0.012 ± 0.006
Heart	0.006 ± 0.001
Kidney	0.005 ± 0.001
Lower large intestine	0.004 ± 0.003
Red marrow	0.003 ± 0.001
Remainder of body	0.195 ± 0.039

Residence Time and Absorbed Dose Calculations

Time–activity curves (without decay correction) were formed from the subsampled data in each region. For each ROI, the area under the curve to infinity (AUC) representing the cumulated activity per milliliter was computed. Regions displaying monotone

TABLE 3
Radiation-Absorbed Dose Estimates

Organ	mGy/MBq	rad/mCi
Adrenal	3.17E−03	1.17E−02
Brain	3.44E−03	1.27E−02
Breast	1.70E−03	6.28E−03
Gallbladder wall	3.15E−02	1.17E−01
Lower large intestine wall	6.15E−03	2.28E−02
Small intestine	2.58E−02	9.55E−02
Stomach	2.59E−03	9.59E−03
Upper large intestine wall	5.22E−03	1.93E−02
Heart wall	4.06E−03	1.50E−02
Kidney	6.78E−03	2.51E−02
Liver	1.77E−02	6.56E−02
Lung	1.14E−02	4.21E−02
Muscle	2.00E−03	7.40E−03
Ovary	3.91E−03	1.45E−02
Pancreas	3.23E−03	1.19E−02
Red marrow	2.26E−03	8.35E−03
Bone surface	2.00E−03	7.39E−03
Skin	1.42E−03	5.25E−03
Spleen	2.17E−03	8.04E−03
Testis	1.60E−03	5.93E−03
Thymus	1.97E−03	7.28E−03
Thyroid	1.57E−03	5.79E−03
Urinary bladder wall	1.35E−02	5.00E−02
Uterus	3.90E−03	1.44E−02
Total body	2.83E−03	1.05E−02
	mSv/MBq	rem/mCi
Effective dose equivalent	8.73E−03	3.23E−02
Effective dose	6.26E−03	2.31E−02

decreases in activity were fitted to either mono- or biexponential functions. For all other regions, the AUC was computed as the trapezoidal sum of the observed data plus pure physical decay (the most conservative assumption) for the tail portion after the end of the scanning data.

The computed AUCs were normalized to the injected activity, corrected for scanner-to-dose calibrator calibration. For organs other than urinary bladder, the resulting integrals (h/cm^3) were multiplied by the organ volumes as computed for the 70-kg adult mathematic phantom (*23*) to obtain residence times (h). The AUC for urinary bladder represented total cumulated activity for that organ. For small intestine, the conservative assumption was made that mean activity equaled that observed in duodenum, so that the residence time for this organ was likely to be somewhat overestimated. The fraction of total activity not attributed to sampled organs was assigned to a remainder of the body term.

Residence times for each subject were entered into MIRDOSE3.1 software (*24*) to compute subject-wise absorbed doses. A voiding model was not used for the urinary bladder—that is, the conservative assumption was made that the first voiding cycle

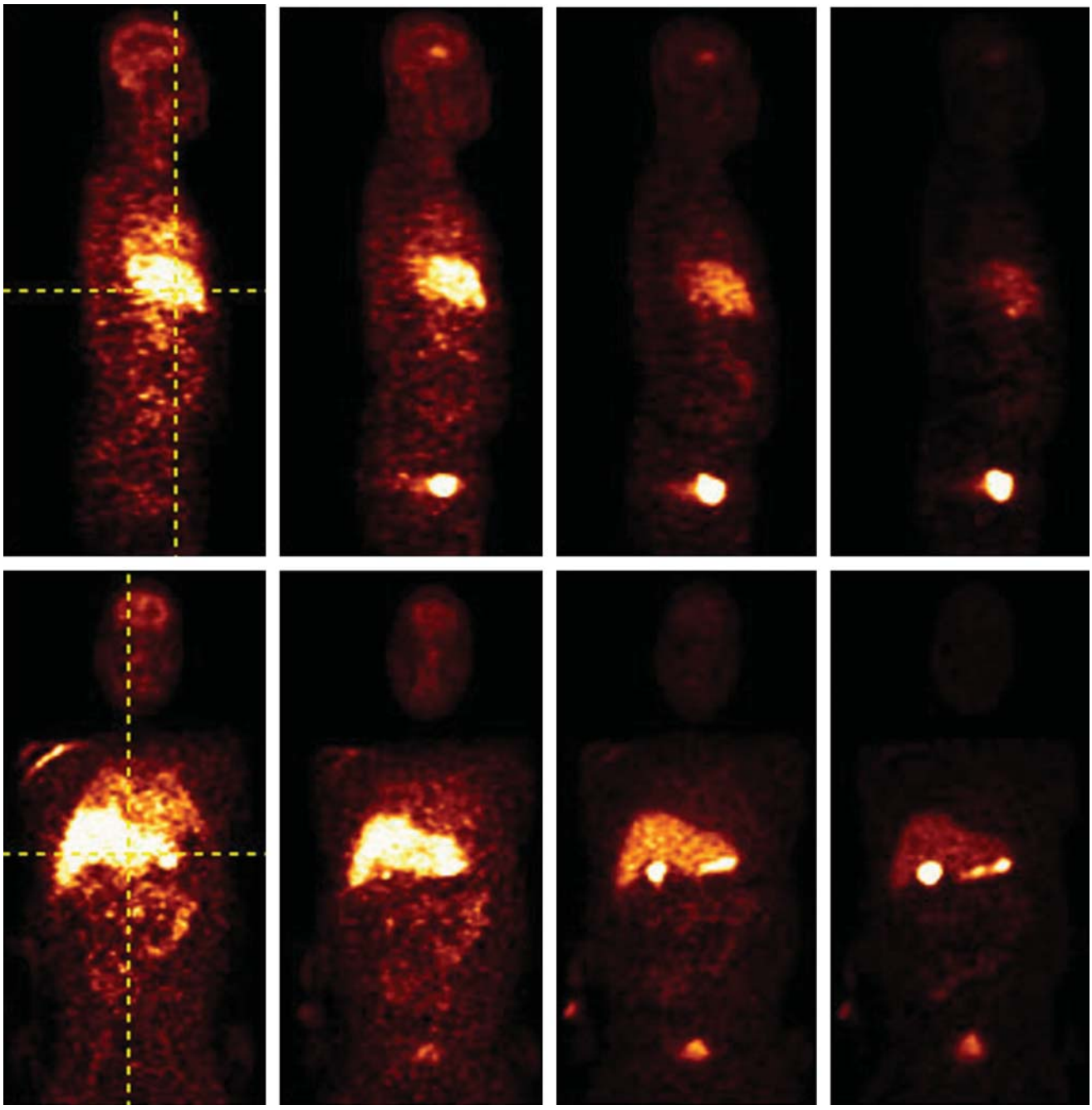

FIGURE 1. Sagittal (top row) and coronal (bottom row) views of whole-body images in 1 healthy human subject at 1, 10, 20, and 40 min after injection of ^{11}C-raclopride. Vertical crosshair in sagittal view shows the slice level of coronal images. Vertical crosshair in coronal view shows the slice level of sagittal images. Initial uptake is predominantly in liver but eventually settles in gallbladder and urinary bladder (compare with Fig. 2). Note prominent uptake in striatum (brain) at 10 and 20 min.

would occur after negligible activity was remaining in the bladder. Similarly, a gastrointestinal transit model was not used. Organ absorbed doses, effective dose, and effective dose equivalent were computed as the mean of these quantities across the 6 subjects.

RESULTS

Mean residence times are displayed in Table 2. Organ absorbed doses, effective dose equivalent, and effective dose are displayed in Table 3. For most subjects, heart, kidney, and lung were monotone decreasing, whereas small intestine and urinary bladder were unimodal, reaching peak value approximately 20 min after injection. Gallbladder was multimodal (decreasing activity for approximately 15–20 min, followed by increasing activity to peak between 40 and 50 min, followed by rapid decrease for the remainder of the scan) in all 6 subjects (Figs. 1 and 2). The dose-limiting organ (organ with largest absorbed dose) was the gallbladder (3.16×10^{-2} mGy/MBq)

DISCUSSION

In this study, radiation dosimetry of ^{11}C-raclopride was estimated from data acquired with whole-body PET in 6 human subjects. It was observed that the organ with the largest absorbed dose was the gallbladder wall (0.0317 mGy/MBq or 0.117 rad/mCi). U.S. federal regulations for studies performed under Radiation Drug Research Committee (RDRC), as specified in *Title 21 CFR 361.1* (*25*), state that the maximal absorbed doses for active blood-forming organs, whole body, lens of eye, or gonad are 3 rem per single study, or 5-rem annual and total dose commitment. For all other organs, the limits are 5 rem per single study and 15-rem annual and total dose commitment. Using the data presented here, gallbladder is the dose-limiting organ, with limits equal to 1.58 GBq (42.8 mCi) injected dose per single study, or 4.75 GBq (128 mCi) annually.

In a recently published study of ^{11}C-raclopride whole-body dosimetry in humans (*20*), kidney was observed to be the dose-limiting organ (0.0406 ± 0.0331 mGy/MBq), leading to a slightly lower dose limit (1.22 GBq [33 mCi] for a single study) if the above criteria are applied. Though this is well above the 370–555 MBq (10–15 mCi) typically used in single-bolus studies, it is puzzling that the 2 studies in humans measured activities of different orders of magnitude in kidney. The studies differed in several aspects of methodology and instrumentation (Table 4). For kidney in this study, frames 1 and 2 were acquired 2.25 and 6.6 min after injection. Assuming, as with this study, that kidneys were located in bed position 4 in Ribeiro et al. (*20*) and that scanning commenced immediately after injection, frames 1 and 2 would have been acquired at 3.5 and 12.2 min after injection. Thus, early activity in kidney, an organ with rapid washout (Fig. 2), was more directly measured in this study. Because absorbed doses were published for each of the 3 subjects in Ribeiro et al. (0.0247, 0.0185, and 0.0787 mGy/MBq), it is possible to directly compare the reproducibility of the kidney estimates in the 2 human studies. A 95% confidence interval for kidney absorbed dose in Ribeiro et al. is from −0.0416 to 0.1229 mGy/MBq—that is, the interval extends below 0 and is approximately 400% of the estimated mean; the 95% confidence interval for the present study is from 0.0055 to 0.0080

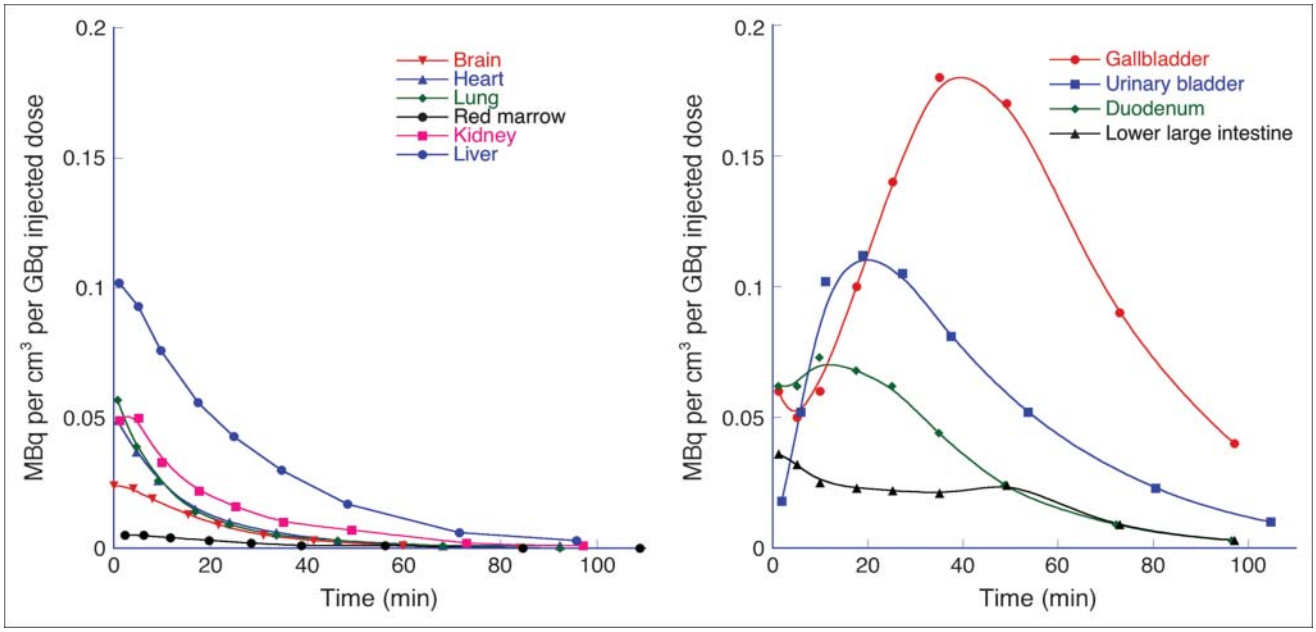

FIGURE 2. Time–activity curves for all organs. Units are activity concentration (MBq/cm^3) normalized to injected dose (GBq). (A) Low- and moderate-uptake organs. (B) High-uptake organs (urinary bladder contents concentration is taken from a central subsample for comparability with other organs). Markers are average of measured data, interpolated to the same time for each organ (timing varied slightly from subject to subject). Fitted curves are for display and do not represent a physiologic model.

TABLE 4
Comparison of Instrumentation and Several Scanning Parameters Between This Study and the Study of Ribeiro et al. (*20*)

Comparison	This study	Study of Ribeiro et al. (*20*)
Scanner	Accel	HR+
Acquisition/ reconstruction	2-dimensional	3-dimensional
Transmission scan duration	5 min per bed	3 min per bed
Frame duration per bed	15 s to 2 min	1 min
Scan starting time	1 min after injection	Not specified

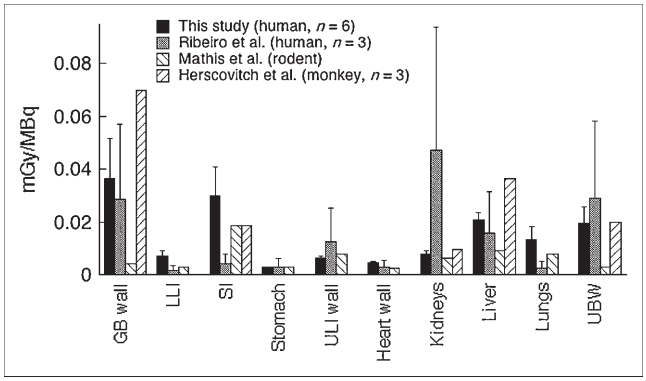

FIGURE 4. Comparison of radiation-absorbed doses from this study with other studies (*18–20*). Units are mGy/MBq. Error bars are SD (not available for rodent and monkey studies). GB = gallbladder; LLI = lower large intestine; SI = small intestine; ULI = upper large intestine; UBW = urinary bladder wall.

mGy/MBq, or 37% of the estimated mean. While this demonstrates that measurement of kidney activity was less variable in this study, it is noteworthy that all 3 subjects in Ribeiro et al. exceeded the mean of this study in kidney by approximately 3-fold or more. Therefore, we examined the possibility that the organ subsampling procedure used here may have led to artifactually low estimates in kidney if highly localized hot spots were missed. To test this, larger kidney ROIs encompassing the entire organ were drawn. Though this approach may be more susceptible to partial-volume spillover or contamination from improperly included adjacent tissues, any localized hot spots missed by the subsampling method would be included. Computed residence times for the more inclusive kidney regions were 108% ± 13% of those using the subsampling technique. Thus, it does not appear that kidney doses were grossly underestimated because of missed activity in the present study (Fig. 3). Figure 4 compares absorbed dose calculations from all 4 studies (the present study and (*18–20*)) in several organs. Although differences due to methodology and species are to be expected—for example, rats do not have a gallbladder (*26*), so that rat studies either have no self-dose for that organ or require an approximation based on a biliary excretion model and measurements from small intestine (*27*)—we do note that the measured activity in kidney in both animal studies was similar in the order of magnitude to that of the present study and that activities in the nonhuman primate study were of similar order of magnitude to that of the present study in all organs reported in both studies. Nonetheless, results obtained in humans are the most relevant to radiation safety in humans, and it remains for future work to definitively identify the source of the discrepancy between this study and the study of Ribeiro et al. in kidney.

In this study, a urinary voiding model was not used. This choice was based on the nature of the data and the scanning protocols that are commonly used with ^{11}C-raclopride. Subjects were scanned for approximately 110 min, or 5.4 half-lives of ^{11}C. At the end of that time, <3% of the injected activity remains throughout the whole body. In particular, the time–activity curves in the urinary bladder decayed to negligible amounts (Fig. 2), making it possible to estimate the bladder contents' residence time directly from the observed data. While the duration of these scans may be longer than a typical voiding cycle, many of the

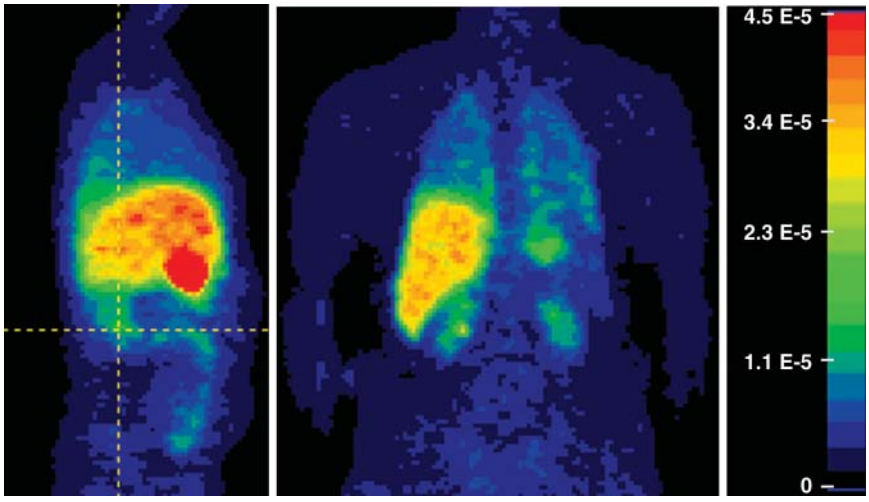

FIGURE 3. Weighted summation of dynamic data from 1 subject. Frames were weighted by the pass durations so the summation represents an approximation to a residence time density image. Units are h/cm^3. Color scale was truncated at 4.5×10^{-5} h/cm^3 (right) so that high-uptake (gallbladder) and low-uptake (kidney) organs could be visualized in same image—that is, all values $\geq 4.5 \times 10^{-5}$ h/cm^3 are mapped to same color (red). Vertical gridline on sagittal (left, facing to right) view shows slice level of coronal view (center), at level of kidney.

^{11}C-raclopride scans that are performed currently and for the foreseeable future are research scans. It is not uncommon for such scans to have durations of 90 min or more, so that the conditions in this study were similar to those in common usage with this radiotracer. Regardless of scan duration, the urinary bladder wall was ultimately not the dose-limiting organ. The estimated absorbed doses in organs that are in proximity to the bladder (0.00391 mGy/MBq in ovary, 0.00160 mGy/MBq in testis) are still orders of magnitude less than those in gallbladder, liver, and small intestine—organs that are, at most, nominally affected by activity in urinary bladder due to physical distance. Thus, for this radiotracer, a voiding model would not materially change the estimation of radiation burden.

Recently, radiation dosimetry estimates derived from PET studies performed in human volunteers were reported for the serotonin transporter ligand ^{11}C-labeled 3-amino-4-(2-dimethylaminomethylphenylsulfanyl)benzonitrile (^{11}C-DASB) (*28*). In that study, coronal slices were summed (i.e., anterior to posterior) and ROIs were drawn on the resulting 2D projection images, encompassing entire organs and some surrounding tissue. A previous ^{11}C-DASB whole-body dosimetry study in nonhuman primates from the same laboratory (rhesus monkey, $n = 2$) (*29*) compared this approach to activity estimation with one using samples drawn on tomographic (i.e., 3-dimensional) data with ROIs carefully delineating organs (to the extent possible with visual inspection) and found the 2 methods comparable. In the present study, we chose to use a subsampling approach in all organs other than urinary bladder. This was because of the close spatial proximity of high-activity organs. Boundaries between these organs were found to be difficult to assess on ^{11}C-raclopride images. Additionally, near the boundaries there is likely to be cross-contamination between organs because of partial-volume effect. The subsampling approach avoids these difficulties but requires the assumption that ^{11}C-raclopride and its radiolabeled metabolic by-products are approximately homogeneously distributed in the sampled organs. This assumption appears reasonably well satisfied in the present dataset. As in the present study, it was observed in the report of Lu et al. (*28*) that allowable doses based on human data were somewhat different than those obtained from studies of rodents (*30*) as well as nonhuman primates (*29*). These studies highlight the importance of obtaining dosimetry estimates in humans for PET ligands that will ultimately be used in research with human subjects.

CONCLUSION

Absorbed dose estimates for ^{11}C-raclopride obtained in 6 human subjects demonstrated gallbladder to be the dose-limiting organ (allowable single dose = 1.58 GBq [42.3 mCi]). This is in contrast to a recent study in 3 humans that found kidney to be the dose-limiting organ, but the maximal doses suggested by both studies are still several times larger than the 370- to 555-MBq (10–15 mCi) doses commonly used with this ligand in PET.

ACKNOWLEDGMENTS

This work was supported by NIMH grants 5 P50 MH066171-02, 1-K02-MH01603-01, the Lieber Center for Schizophrenia Research at Columbia University, and the New York State Office of Mental Health.

REFERENCES

1. Ehrin E, Farde L, de Paulis T, et al. Preparation of ^{11}C-labelled raclopride, a new potent dopamine receptor antagonist: preliminary PET studies of cerebral dopamine receptors in the monkey. *Int J Appl Radiat Isot.* 1985;36:269–273.
2. Dewey SL, Smith GS, Logan J, et al. Striatal binding of the PET ligand ^{11}C-raclopride is altered by drugs that modify synaptic dopamine levels. *Synapse.* 1993;13:350–356.
3. Laruelle M. Imaging synaptic neurotransmission with in vivo binding competition techniques: a critical review. *J Cereb Blood Flow Metab.* 2000;20:423–451.
4. Small DM, Jones-Gotman M, Dagher A. Feeding-induced dopamine release in dorsal striatum correlates with meal pleasantness ratings in healthy human volunteers. *Neuroimage.* 2003;19:1709–1715.
5. Koepp MJ, Gunn RN, Lawrence AD, et al. Evidence for striatal dopamine release during a video game. *Nature.* 1998;393:266–268.
6. Antonini A, Schwarz J, Oertel WH, et al. [^{11}C]Raclopride and positron emission tomography in previously untreated patients with Parkinson's disease: influence of L-dopa and lisuride therapy on striatal dopamine D2-receptors. *Neurology.* 1994;44:1325–1329.
7. Piccini P, Brooks D, Bjorklund A, et al. Dopamine release from nigral transplants visualized in vivo in a Parkinson's patient. *Nat Neurosci.* 1999;2:1137–1140.
8. Rinne JO, Laihinen A, Rinne UK, et al. PET study on striatal dopamine D2 receptor changes during the progression of early Parkinson's disease. *Mov Disord.* 1993;8:134–138.
9. Tedroff J, Pedersen M, Aquilonius SM, et al. Levodopa-induced changes in synaptic dopamine in patients with Parkinson's disease as measured by [^{11}C]raclopride displacement and PET. *Neurology.* 1996;46:1430–1436.
10. Breier A, Su TP, Saunders R, et al. Schizophrenia is associated with elevated amphetamine-induced synaptic dopamine concentrations: evidence from a novel positron emission tomography method. *Proc Natl Acad Sci U S A.* 1997;94:2569–2574.
11. Farde L, Wiesel FA, Halldin C, et al. Central D2-dopamine receptor occupancy in schizophrenic patients treated with antipsychotic drugs. *Arch Gen Psychiatry.* 1988;45:71–76.
12. Hietala J, Syvälahti E, Vuorio K, et al. Striatal D2 receptor characteristics in neuroleptic-naive schizophrenic patients studied with positron emission tomography. *Arch Gen Psychiatry.* 1994;51:116–123.
13. Barrett SP, Boileau I, Okker J, et al. The hedonic response to cigarette smoking is proportional to dopamine release in the human striatum as measured by positron emission tomography and C-11 raclopride. *Synapse.* 2004;54:65–71.
14. Boileau I, Assaad JM, Pihl RO, et al. Alcohol promotes dopamine release in the human nucleus accumbens. *Synapse.* 2003;49:226–231.
15. Kaasinen V, Aalto S, Nagren K, et al. Expectation of caffeine induces dopaminergic responses in humans. *Eur J Neurosci.* 2004;19:2352–2356.
16. Martinez D, Broft A, Foltin RW, et al. Cocaine dependence and D-2 receptor availability in the functional subdivisions of the striatum: relationship with cocaine-seeking behavior. *Neuropsychopharmacology.* 2004;29:1190–1202.
17. Volkow ND, Wang GJ, Fowler JS, et al. Brain DA D2 receptors predict reinforcing effects of stimulants in humans: replication study. *Synapse.* 2002;46:79–82.
18. Mathis CA, Simpson NR, Blastos BP, et al. Biodistribution and dosimetry estimates of [C-11]raclopride [abstract]. *J Nucl Med.* 1996;37(suppl):231P.
19. Herscovitch P, Schmall B, Doudet DJ, et al. Biodistribution and radiation dose estimates for [C-11]raclopride [abstract]. *J Nucl Med.* 1997;38(suppl):224P.
20. Ribeiro M, Ricard M, Bourgeois S, et al. Biodistribution and radiation dosimetry of [^{11}C]raclopride in healthy volunteers. *Eur J Nucl Med Mol Imaging.* 2005;32:952–958.
21. Jewett D. A simple synthesis of [^{11}C]methyl triflate. *Int J Rad Appl Instrum [A].* 1992;43:1383–1385.

22. Tarantola G, Zito F, Gerundini P. PET instrumentation and reconstruction algorithms in whole-body applications. *J Nucl Med.* 2003;44:756–769.
23. Cristy M, Eckerman K. *Specific Absorbed Fractions of Energy at Various Ages from Internal Photon Sources.* Oak Ridge, TN: Oak Ridge National Laboratory; 1987.
24. Stabin M. MIRDOSE: personal computer software for internal dose assessment in nuclear medicine. *J Nucl Med.* 1996;37:538–546.
25. Food and Drug Administration. *Title 21 CFR 361.1, Radioactive Drugs for Certain Research Uses.* 4-1-01 ed. Washington, DC: National Archives and Records Administration; 2001:300–305.
26. Gaudio E, Onori P, Pannarale L, et al. Microcirculation of the extrahepatic biliary tree: a scanning electron-microscopy study of corrosion casts. *J Anat.* 1993;182:37–44.
27. Wrobel M, Carey J, Sherman P, et al. Simplifying the dosimetry of carbon-11-labeled radiopharmaceuticals. *J Nucl Med.* 1997;38:654–660.
28. Lu J, Ichise M, Liow J, Ghose S, Vines D, Innis R. Biodistribution and radiation dosimetry of the serotonin transporter ligand ^{11}C-DASB determined from human whole-body PET. *J Nucl Med.* 2004;45:1555–1559.
29. Tipre DN, Lu JQ, Fujita M, Ichise M, Vines D, Innis RB. Radiation dosimetry estimates for the PET serotonin transporter probe ^{11}C-DASB determined from whole-body imaging in non-human primates. *Nucl Med Commun.* 2004;25: 81–86.
30. Wilson AA, Ginovart N, Hussey D, Meyer J, Houle S. In vitro and in vivo characterization of ^{11}C-DASB: a probe for in vivo measurements of the serotonin transporter by positron emission tomography. *Nucl Med Biol.* 2002; 29:509–515.